Article

Theoretical investigation of the vibrational structure of the Ar–CO$_2$ complex

Olaseni Sode [*], Jesus Ruiz, Steve Peralta

Department of Chemistry and Biochemistry, California State University, Los Angeles, 5151 State University Drive, Los Angeles, 90032, USA

ARTICLE INFO

ABSTRACT

We develop a new flexible-monomer two-body *ab initio* potential energy surface (PES) for the Ar–CO$_2$ complex. The accuracy of this new potential function is validated by its agreement in the vibrational spectrum of the complex. Vibrational self-consistent field theory (VSCF) and vibrational configuration interaction (VCI) theory were employed to solve the complete vibrational Hamiltonian, including both intermolecular and intramolecular degrees of freedom. We observe excellent agreement with theoretical and experimental results for the vibrational energy levels in the Terahertz region. In the intramolecular region, we confirm the slight splitting of the bending modes of the CO$_2$ monomer, where the in-plane bend is 0.83 cm$_{-1}$ less energetic than the out-of-plane mode. We also explore the combination bands in the asymmetric stretching region of the CO$_2$ monomer that involve the intermolecular motions, and show that these results compare favorably to the fundamental intermolecular vibrational energy levels.

1. Introduction

Due to its importance in atmospheric and environmental chemistry, the carbon dioxide molecule and its van der Waals complexes have been the focus of numerous experimental and theoretical studies [1–5]. In particular, the argon–carbon dioxide complex has been of interest since it represents the model system for these weak, yet non-trivial interactions. The minimum energy structure for the Ar–CO$_2$ complex has been determined experimentally to be the classic T-shaped structure with C_{2v} symmetry [6]. Recently, a linear structure was also been found with a theoretical approach [7]. Vibrational spectroscopy represents an invaluable technique for analyzing the potential energy surface (PES) and dynamics of such chemical complexes, given its sensitivity to these specific types of interactions. Further, for probing the interactions that occur within molecules, infrared spectroscopy is ubiquitous and essential. It can even be used to explore the intermolecular interactions through combination bands in the intramolecular region of the vibrational spectrum.

The vibrational frequencies for the Ar–CO$_2$ complex show characteristic differences compared to the isolated carbon dioxide molecule. In the monomer system, the four fundamental vibrational motions – two degenerate bending modes, a symmetric stretch and an asymmetric stretch – have been precisely and extensively studied by experimentalists and theoreticians alike [8–20]. Also, of particular interest in the vibrational spectrum is the familiar Fermi resonance, or the accidental degeneracy of the symmetric stretch fundamental and the overtone of the degenerate bending modes, which is observed through Raman spectroscopy [21–26]. For the argon complex, an overwhelming amount of

research is focused on the van der Waals interactions [27–31]. Here, two fundamental vibrations, the intermolecular bending mode and the intermolecular stretching mode are observed experimentally with energies of 27.818 cm^{-1} and 37.5 cm^{-1}, respectively [6,28]. Recent theoretical investigations have confirmed these results [7,32]. Yet until recently, few studies examined the intramolecular frequency shifts in the complex [33]. One such recent experimental study explored the intramolecular bending frequencies for the complex and observed a slight symmetry breaking for the modes in the monomer due to the presence of the Ar atom [34]. This splitting amounted to about a 0.87 cm^{-1}, where, using experimental and simulated rotational spectroscopy, they observed the in-plane bend as slightly lower in energy than the out-of-plane motion.

In order to correctly describe such fine vibrational structure, an accurate potential energy surface is critical. Previously, we employed permutationally invariant polynomials fit to electronic structure energies calculated at the CCSD(T) level of theory and aug-cc-pVTZ basis set to develop a one-body carbon dioxide monomer potential energy function (PEF), as well as a flexible-monomer two-body carbon dioxide dimer potential [35]. Combined, these two PEFs were implemented to determine the stable isomers for clusters of CO$_2$ molecules up to and including the tridecamer [35]. Additionally, the accuracy of the PEFs was confirmed through vibrational structure computations of the CO$_2$ monomer, dimer and two trimer isomers (i.e., the barrel-shaped and cyclic trimers) [36]. In the case of the monomer and dimer, our previous data agreed quite well with the vast amount of experimental

---

band assignments and energy levels. This agreement was extended even to the Fermi dyad peaks in both the monomer and dimer [20]. For the cyclic trimer, we were able to reassign a pair of intermolecular vibrational motions that were previously incorrectly ordered based on experimental observations. For the barrel-shaped isomer, we presented the first theoretical or experimental exploration of the vibrational modes using these new PEFs.

The choice of vibrational structure approach also plays an important role in the accuracy of the theoretical vibrational energy levels. Often, a hierarchy of vibrational structure methods – including the harmonic approximation, vibrational self-consistent field (VSCF) theory, and vibrational configuration interaction (VCI) theory – is applied [37]. This choice amounts increasingly rigorous solutions to the vibrational Hamiltonian. The accurate PEF and hierarchical vibrational structure methods can be used to simulate the vibrational spectrum of the chemical system. In this article, we develop a new flexible-monomer two-body PES using a model function constructed from permutationally invariant polynomials. This function is trained against *ab initio* energies of the $Ar--CO_2$ complex. We then integrate this potential function into the vibrational Hamiltonian and determine the vibrational energy levels solved at the VSCF and VCI levels of theory.

2. Computational details

2.1. Potential energy surface

The potential energy function (PEF) used in the present work was constructed using permutationally invariant polynomials fit to the electronic energies of the carbon dioxide monomer and the argon−carbon dioxide dimer. Previously, we developed the one-body PEF for the CO_2 monomer using a sixth-degree symmetrized polynomial function fit to over 170,000 configurations of CO_2 monomers computed at the CCSD(T)-F12b level of theory with the aug-cc-pVTZ basis set [35]. This combination of theory and basis set approaches the most accurate theoretical computations for the molecule. In the current work, we develop the two-body PEF for the $Ar−CO_2$ dimer by employing a fifth-degree polynomial function consisting of intramolecular and intermolecular exponential functions for each of the six interatomic distances in the complex. Nonlinear coefficients (k) for unique interatomic interactions were also included in the exponential functions below:

$$\xi_{intra} = e^{k_{intra} \cdot d} \tag{1}$$

$$\xi_{inter} = e^{k_{inter} \cdot d} / d. \tag{2}$$

The fifth-degree function built from a linear combination of 222 unique symmetrized polynomials was generated from these exponentials, along with linear coefficients. Thus the two-body potential not only accounts for the intermolecular dynamics in the $Ar−CO_2$ complex, but also for the intramolecular degrees of freedom of the CO_2 molecule. The entire function can be found in the authors' GitHub repository.

A training set of 66,336 unique $Ar−CO_2$ configurations was computed at the CCSD(T)-F12b/aug-cc-pVTZ level of theory and basis set with the Molpro software package [38]. The training set was generated using a three-dimensional grid (the grid parameters included the intermolecular distance, the intermolecular bend angle, and the intramolecular carbon–oxygen distance), projections along the normal and combination modes of vibrations from the global minimum energy (T-shaped) structure, and random configurations where both the intermolecular and intramolecular parameters were varied. The shortest argon–carbon distance in the training set was 2.5 Å and the longest distance was 6.0 Å. The most repulsive configuration had an interaction energy of 492.2 kcal mol^{-1}. All of the configurations can be found in the authors' GitHub repository.

This training set was used to fit the flexible-monomer two-body PEF. Linear and non-linear coefficients were optimized via Tikhonov
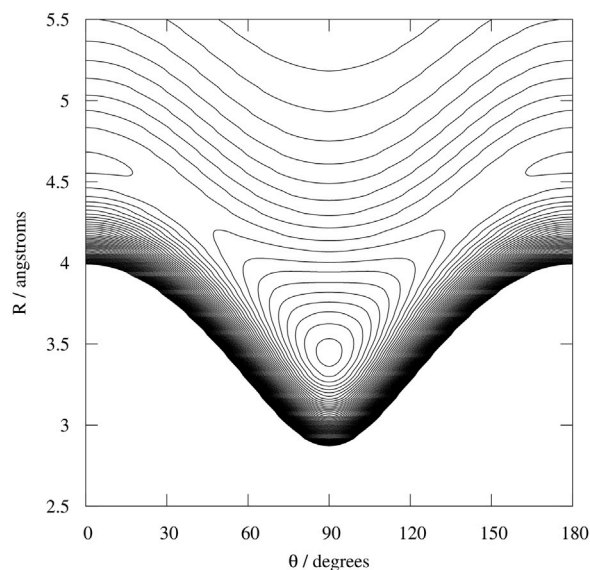

Fig. 1. The intermolecular potential energy surface of the $Ar–CO_2$ complex is shown with a contour spacing of 10 cm^{-1}. The minimum energy (-195.96 cm^{-1}) structure is located at $R = 3.436$ Å and $\theta = 89.99°$. Intramolecular CO_2 bond distances are held fixed.

regularization,[39] minimizing the weighted sum of the squared errors according to the following equation:

$$\chi^2 = \sum_n w_n \left[V^{model}(n) - V^{ref}(n) \right]^2 + \Gamma \sum_k c_k^2. \tag{3}$$

Here, k runs over the list of linear coefficients, n runs over the list of training set configurations, and Γ represents the regularization term, set to 5.0×10^{-2}, which mitigates overfitting. The model and reference energies for the nth configuration are given as $V^{model}(n)$ and $V^{ref}(n)$, respectively. The weighting factor (w_n), which stresses configurations with lower total energies, is expressed as:

$$w(E) = \left(\frac{\Delta E}{E - E_{\min} + \Delta E} \right)^2, \tag{4}$$

where $E_{\min}$ is the minimum energy value, and ΔE, set to 10 kcal mol^{-1}, is the energy range for selecting the subset of emphasized configurations.

The fit of the model potential, shown in Table 1 is strikingly accurate with respect to the reference energies, especially in the low-energy range. The optimized linear and nonlinear parameters resulted in a χ^2 value of 5.2600 (kcal mol^{-1})^2 and a mean absolute error of 6.362 cm^{-1}. The largest deviation from the training set energies within the low-energy range was 37.5813 cm^{-1}. The optimized model potential was compared to a test set 11,533 configurations. The resulting agreement between the model energies and the test set energies is also shown in Table 1. Notably, the root mean squared error, mean absolute error, and maximum error were comparable in the training and the test sets.

2.2. Vibrational Schrödinger equation

The argon−carbon dioxide complex PES is included in the vibrational Hamiltonian with general curvilinear coordinates. This Hamiltonian is separable and can be decomposed into its kinetic energy and potential energy terms [40,41]. In this article, we employ the notation introduced by Strobusch and Scheurer [40,41] to refer to the many-body expansion orders for Hamiltonian terms, as $V(O_V)/T(O_M, O_K, O_{\nabla G}, O_{V_g})$. These components refer to the potential energy term (V), on-diagonal (M) and off-diagonal (K) elements of the kinetic energy operator G matrix terms, the ∇G term, and the pseudo-potential term, commonly denoted as V_g. For the $Ar−CO_2$ complex, we employ a

Table 1

The fitting accuracy for the Ar−CO_2 two-body energy function. The root mean squared error (RMSE), mean absolute error (MAE), and maximum errors (MAX) are shown over the entire training and test set and for the low-energy configurations of each in units of cm^{-1}. The χ^2 value has units of (kcal mol^{-1})^2. The low parameters only include structures with energies within the ΔE range. The RMS errors, mean absolute errors and maximum errors are given in kcal mol^{-1}, and the χ^2 term has units of (kcal mol^{-1})^2.

	Configs.	RMSE	RMSE low	MAE	χ^2	MAX	MAX low
Training set	66,336	36.2628	1.45303×10^{-2}	6.362	5.2600	1525.74	37.5813
Test set	11,533	42.4325	3.03390×10^{-3}	6.705	–	1511.16	41.4812

reduced-dimensional vibrational Hamiltonian, V(3)/T(3,3,3,3). At the VSCF level, this reduced-dimensional Hamiltonian is nearly exact compared to the full expansion, V(6)/T(6,6,6,6,6). Because of the accuracy in the vibrational Hamiltonian and the simultaneous consideration of the intermolecular and intramolecular degrees of freedom, our approach in this work is unique and an improvement over other theoretical procedures.

To solve the vibrational Schrödinger equation, the vibrational self-consistent field (VSCF) [42–45] and the vibrational configuration interaction (VCI) approaches [46–48] are employed alongside the harmonic approximation within the NITROGEN software package [49]. The VSCF approach is exact when the Hamiltonian is additively separable and defines solutions to the Schrödinger equation wavefunctions as products of one-mode functions. The VCI calculations allow for the explicit consideration of mode-mode interactions, which can be quantified through evaluating the contributions to the wavefunctions. In this work, only configurations with a maximum sum of VCI quanta less than fifteen (a total of 38,760 VSCF configurations) were considered. At this level, the vibrational frequencies are well converged. Excited state energies and VCI configuration amplitudes can be found in the authors' GitHub repository (http://github.com/sodelab).

3. Results and analysis

3.1. Structural parameters

The global minimum for the Ar−CO_2 complex is T-shaped and is located at an argon−carbon distance of $R = 3.436$ Å, an argon−carbon−oxygen angle of $\theta = 89.99°$, and an intramolecular carbon−oxygen distance of $r_{CO} = 1.1622$ Å, with a well depth of −195.9603 cm^{-1}. This minimum is observed near the middle of Fig. 1. The authors' GitHub repository includes the global minimum geometry, whose values are also listed in Table 2, alongside theoretical and experimental results from the literature for comparison. We compare our optimized Ar−CO_2 structural parameters to those obtained from potential energy functions developed by Cui et al. [32] and Zhao et al. [7], which show good overall agreement with the global minimum energy structure. The theoretical structural parameters refer to the equilibrium structure , but the experimental structural parameters refer to the zero-point energy structure. This helps explain the slight discrepancy between the theoretical and experimental results. A second energy-minimum is found at the edges of Fig. 1 and has a linear geometry. Here, the intermolecular distance between the carbon and argon atoms is equal to 4.620 Å, and the well depth is −115.4254 cm^{-1}. For the linear structure, the two intramolecular r_{CO} bonds are nearly identical, with a bond length of 1.1623 Å. This distance is slightly longer than the intramolecular bond lengths in the T-shaped complex and in the isolated CO_2 monomer, which we have previously shown to have an intramolecular bond distance of 1.1622 Å [20].

3.2. Intermolecular vibrational frequency region

The frequencies for the first five intermolecular vibrations, along with their assignments, for the T-shaped Ar−CO_2 complex are presented in Table 3. Two fundamental vibrations are observed in this region: the intermolecular bend (v_b) and the van der Waals stretch (v_s). We observe the bend fundamental as the lowest vibrational excitation at all levels of

Table 2

The structural parameters of the ground state minimum of the Ar−CO_2 complex. The experimental parameters refer to the zero-point energy structure, while the other theoretical parameters are for the minimum-energy structure.

	R	θ	r_{CO}	Energy
Cui et al. [32]	3.440	90.0	–	−200.97
Zhao et al. [7]	3.432	90.0	–	−199.38
This work	3.436	89.99	1.1622	−195.96
Experiment [6]	3.5032	82.95		

theory. And, as the level of theory increases and more anharmonicity is accounted for, this vibrational frequency decreases to 27.08 cm^{-1} with the VCI method. This value agrees well with the experimental value of 27.818 cm^{-1} for the intermolecular bend vibration. The stretch fundamental vibration is more energetic, and likewise shows a decrease in energy as the vibrational structure approach is improved. The VCI frequency is computed at 33.61 cm^{-1}. No direct experimental measurement exists for this mode; however, an experimental estimate places this frequency at 37.5 cm^{-1}, slightly higher than our VCI value [6]. Our results more closely agree with the theoretical excitation energies obtained by Cui et al. [32] and Zhao et al. [7], shown in Table 3, which are both around 34 cm^{-1}. Given the estimated nature of the experimental result for this mode, the theoretical predictions are likely closer to the true value. Furthermore, it should also be noted that the experimental frequencies in this region were only observed by exploring combination bands in the CO_2 asymmetric stretch region, which we will discuss later.

Three combination and overtone vibrations, also found in the intermolecular region of the complex, are shown in Table 3. In increasing energy, they are the intermolecular bend overtone ($2v_b$), the bend and stretch combination ($v_b + v_s$), and the van der Waals stretch overtone ($2v_s$). With VCI, the vibrational frequencies relax compared to VSCF and are found at 51.60, 53.12 and 62.73 cm^{-1}, respectively. Again, these results agree well with the previous theoretical spectra proposed by of Cui et al. and Zhao et al. although our frequencies are slightly less energetic than theirs by no more than about 1 cm^{-1}. The VCI coefficients for each of these vibrational frequencies can be found in the authors' GitHub repository (http://github.com/sodelab).

3.3. Intramolecular vibrational frequency region

The frequencies in the intramolecular region of the T-shaped Ar−CO_2 complex are presented in Table 4. The first eight frequencies listed in the table belong to the intramolecular vibrations of the CO_2 molecule alone. Four of these represent fundamental modes: the in-plane intramolecular bend (v_2^i), out-of-plane intramolecular bend (v_2^o), symmetric stretch (v_1) and asymmetric stretch (v_3). Additional intramolecular vibrational frequencies – only a few of which are shown – arise due to overtones, combinations and the Fermi resonance of these fundamental vibrations. We also present combination bands consisting of the intermolecular motions discussed in Section 3.2 with the asymmetric stretch fundamental. These values provide a useful comparison to the values from Table 3, especially in the case of experiment. A list of all of the vibrational frequencies in this region is provided in the authors' GitHub repository (http://github.com/sodelab).

The two bending modes, shown in Table 4, are observed to have frequencies around 668 cm^{-1}, at the VCI level. Previously for the isolated monomer, we found the degenerate bending modes at 667.8 cm^{-1}

Table 3
The intermolecular vibrational energy levels (in cm^{-1}) of the Ar–CO$_2$ complex obtained with the harmonic approximation, VSCF, and VCI methods are compared to experimental and theoretical values from the literature. The intermolecular stretch frequency denoted below is not a direct experimental measurement, but instead a theoretical estimation based on the approximate experimental structure.[a]

	HAR	VSCF	VCI	Expt [6,28].	Cui et al. [32]	Zhao et al. [7]
ν_b	33.19	28.98	27.09	27.818	28.074	27.781
ν_s	42.93	37.10	33.61	37.5(7)[a]	34.186	34.012
$2\nu_b$		54.69	51.60		52.857	52.276
$\nu_b + \nu_s$		64.37	53.12		54.040	53.497
$2\nu_s$		69.17	62.73		63.250	62.722

Table 4
The intramolecular vibrational energy levels (in cm^{-1}) of the Ar–CO$_2$ complex obtained with the harmonic approximation, VSCF, and VCI methods. Note that unlike in the isolated CO$_2$ monomer, the bending modes, ν_2^o and ν_2^i, are no longer degenerate. The Fermi dyad bands are denoted.[a] The experimental bending frequencies are obtained by adding the energy splittings [34] to the free CO$_2$ monomer bending frequency [11].[b]

	HAR	VSCF	VCI	Expt [28,34,50].	Zhao et al. [7]
ν_2^i	672.08	669.59	667.60	667.380[b]	
ν_2^o	673.05	670.28	668.43	668.257[b]	
$2\nu_2^o \,/\, 2\nu_2^i$			1284.98[a]		
$2\nu_2^i$		1339.35	1337.47		
$2\nu_2^o$		1340.52	1337.47		
$\nu_2^o + \nu_2^i$		1341.60	1337.46		
ν_1	1352.43	1349.43	1388.72[a]		
ν_3	2394.04	2353.10	2347.88	2348.673	
$\nu_3 + \nu_b$		2382.02	2374.81	2376.491	2376.4910
$\nu_3 + \nu_s$		2390.21	2381.47		2382.685
$\nu_3 + 2\nu_b$		2407.67	2399.50		
$\nu_3 + \nu_b + \nu_s$		2417.41	2401.55		
$\nu_3 + 2\nu_s$		2422.27	2410.80		

at the same level of theory,[20], and they were observed experimentally at 667.380 cm^{-1} [11]. Notably, the bending modes are no longer degenerate in the Ar–CO$_2$ complex, and a slight splitting of the mode frequencies is observed at all levels of theory of about 1.0 cm^{-1}. Additionally, the in-plane bend is less energetic than the out-of-plane bend in all of our calculations, which agrees with a recent experimental investigation on the matter. In this previous work, the in-plane intramolecular bend frequency was observed 0.8773(1) cm^{-1} below the out-of-plane frequency [34]. The bending frequency values in Table 4 are obtained by adding this difference to the energy level of the experimentally determined isolated monomer bending mode. Our current results show the same qualitative and quantitative agreement for the sign and magnitude: at the VCI level, the in-plane frequency is 0.83 cm^{-1} below the out-of-plane frequency.

The remaining fundamental frequencies in the intramolecular region remain mostly unchanged compared to the isolated CO$_2$ monomer. The asymmetric stretch frequency in the complex is detected at 2347.72 cm^{-1} at the VCI level, whereas in the isolated CO$_2$ molecule, this excitation energy is found at 2346.7 cm^{-1} with the same level of theory. Experimentally, the asymmetric stretch fundamental for the complex has a frequency of 2348.673 cm^{-1}, while the frequency for the isolated CO$_2$ monomer is 2349.2 cm^{-1} [11,50]. Notably for the experiment, the trend of the vibrational energies upon complexation is inverted relative to the theoretical results. Even though VCI was applied for both the isolated monomer and the complex, the choice of coordinate frame was different. For the isolated monomer, the vibrational Hamiltonian was solved using Cartesian coordinates, which essentially eliminates the KEO expression compared to the more complicated form of the Hamiltonian involving internal coordinates. For the latter, the KEO must be solved explicitly, and it is likely that this difference in treatment partially explains the inverted relative frequencies. That said, the discrepancy is only a few wavenumbers in magnitude. In the symmetric stretch region with VSCF, the fundamental frequency for the complex is found at 1349.43 cm^{-1}, compared to 1340.4 cm^{-1} in the isolated molecule [20]. Due to mode mixing, there is no experimental comparison for this fundamental frequency, however its Fermi resonance can be explored in detail.

Two Fermi dyad peaks are observed at 1284.98 cm^{-1} and 1388.72 cm^{-1} in the VCI spectrum. These frequencies correspond to the accidental degeneracy of the bending overtones ($2\nu_2^o \,/\, 2\nu_2^i$) with the symmetric stretch fundamental. There also are three other bending overtones (shown at 1337.47 and 1337.46 cm^{-1} in the VCI spectrum), which due to their angular momentum about the molecular axis are less symmetric and thus do not participate in mode splitting. The two Fermi resonance frequencies are nearly unchanged from their values in the isolated monomer, which we previously found to be 1284.7 and 1388.7 cm^{-1} [20]. Clearly the slight splitting of the bending peaks has little to no effect on the Fermi splitting. To confirm this, we show the coefficients of the VCI wavefunction for the Fermi dyads below:

$$\Psi_{\nu_1}^{\mathrm{VCI}} = 0.73\Psi_{\nu_1}^{\mathrm{VSCF}} + 0.47\Psi_{2\nu_2^i}^{\mathrm{VSCF}} + 0.49\Psi_{2\nu_2^o}^{\mathrm{VSCF}} + \cdots, \tag{5}$$

and

$$\Psi_{2\nu_2^i/2\nu_2^o}^{\mathrm{VCI}} = 0.68\Psi_{\nu_1}^{\mathrm{VSCF}} - 0.52\Psi_{2\nu_2^i}^{\mathrm{VSCF}} - 0.51\Psi_{2\nu_2^o}^{\mathrm{VSCF}} + \cdots. \tag{6}$$

These coefficients are strikingly similar to those calculated for the CO$_2$ monomer. The main difference, other than the non-degeneracy of the bending modes, is that the mode contributions for the dyad peaks are swapped. Here for the Ar–CO$_2$ complex, the more energetic dyad ($\Psi_{\nu_1}^{\mathrm{VCI}}$) has more ν_1 character than the less energetic dyad. The opposite is true of the bending modes, which contribute more to the less energetic dyad. For the isolated molecule, we observed the opposite composition. Unfortunately, given the sensitivity of VCI coefficients to the PES, the choice of coordinate frame, and the treatment of the molecular Hamiltonian, broad conclusions are hard to draw from these minute differences.

Since we have for the first time employed the complete PES for the Ar–CO$_2$ complex in the vibrational Hamiltonian, we are able to evaluate the combination bands between the intermolecular and intramolecular interactions, notably in the asymmetric stretching region, shown as the last five vibrational modes in Table 4. These combinations bands can be compared to the intermolecular frequencies in Table 3, once the asymmetric stretch frequency is accounted for. We observe the same ordering of the intermolecular motions in the asymmetric stretching region as in the intermolecular region: ν_b, ν_s, $2\nu_b$, $\nu_b + \nu_s$,

and $2\nu_s$. The resulting frequencies at the VCI level are the following: 26.93, 33.59, 51.62, 53.67, and 62.92 cm^{-1}, respectively. The largest discrepancy between the frequencies in the asymmetric region and the intermolecular region is only about 0.5 cm^{-1}. This data clearly points to the effectiveness of the separate treatment of the intermolecular and intramolecular frequencies for the complex, as well as to the overall accuracy of our PES.

4. Discussion and conclusions

We have presented a new flexible-monomer two-body PES for the Ar$-$CO$_2$ complex fit to the interaction energies of the system evaluated at the CCSD(T)-F12b level of theory with the aug-cc-pVTZ basis set. A T-shaped global minimum and a linear local minimum were found for the complex. The vibrational structure of the T-shaped complex was obtained using a many-body expansion of the vibrational Hamiltonian solved at the VSCF and VCI levels of theory. In the intermolecular region of the vibrational spectrum, the frequencies were accurately reproduced compared to both experiment and previous theoretical results. Also, we presented the first vibrationally correlated treatment of the intramolecular frequencies in the Ar$-$CO$_2$ complex, including the characteristic Fermi resonance and the symmetry breaking of the non-degenerate bending modes. The in-plane bending mode was found to have an energy 0.83 cm^{-1} lower than the out-of-plane bend, which nearly exactly matches with experiment. The remaining fundamental intramolecular vibrations experience relatively small shifts from the isolated CO$_2$ monomer of no more than one wavenumber. Lastly, the intermolecular combination bands in the asymmetric stretch region are only slightly shifted compared to the frequencies in the intermolecular region, which is strong evidence for the viability of the separate treatment of the intermolecular and intramolecular modes in the Ar$-$CO$_2$ complex. Investigations of the van der Waals interactions in similar rare-gas complexes of CO$_2$ are currently underway in our lab.

CRediT authorship contribution statement

Olaseni Sode: Conceptualization, Methodology, Software, Supervision, Writing – original draft, Writing – reviewing and editing. **Jesus Ruiz:** Conceptualization, Investigation. **Steve Peralta:** Validation.

Declaration of competing interest

The authors declare that they have no known competing financial interests or personal relationships that could have appeared to influence the work reported in this paper.

Acknowledgments

Appendix A. Supplementary data

Supplementary material related to this article can be found online at https://doi.org/10.1016/j.jms.2021.111512.

References

[1] E.J. Bohac, M.D. Marshall, R.E. Miller, The vibrational predissociation of Ar–CO2 at the state-to-state level. I. Vibrational propensity rules, J. Chem. Phys. 97 (7) (1998) 4890, http://dx.doi.org/10.1063/1.463951, URL https://aip.scitation.org/doi/abs/10.1063/1.463951.

[2] K.V.J. Jose, S.R. Gadre, An ab initio investigation on (CO2)n and CO2(Ar)m clusters: Geometries and IR spectra, J. Chem. Phys. 128 (12) (2008) 124310, http://dx.doi.org/10.1063/1.2838202, URL https://aip.scitation.org/doi/abs/10.1063/1.2838202.

[3] P. Seal, S. Chakrabarti, Suitability of double hybrid density functionals and their dispersion-corrected counterparts in producing the potential energy curves for CO2-Rg (Rg: He, Ne, Ar and Kr) systems., J. Phys. Chem. A 113 (7) (2009) 1377–1383, http://dx.doi.org/10.1021/jp809341g, URL https://pubs.acs.org/doi/full/10.1021/jp809341g.

[4] L. Wang, D. Xie, Finite temperature path integral Monte Carlo simulations of structural and dynamical properties of ArN–CO2 clusters, J. Chem. Phys. 137 (7) (2012) 074308, http://dx.doi.org/10.1063/1.4746941, URLhttps://aip.scitation.org/doi/full/10.1063/1.4746941.

[5] A. Zhao, L. Shi, Y. Tian, D. Yang, R. Zheng, Investigating the spectroscopic characteristics of twelve isotopologues for the Ar–CO2 complex, J. Quant. Spectrosc. Radiat. Transfer 242 (2020) 106778, http://dx.doi.org/10.1016/j.jqsrt.2019.106778, URL https://www.sciencedirect.com/science/article/pii/S0022407319307691.

[6] J.M. Steed, T.A. Dixon, W. Klemperer, Determination of the structure of ArCO2 by radio frequency and microwave spectroscopy, J. Chem. Phys. 70 (9) (1979) 4095–4100, http://dx.doi.org/10.1063/1.438033, URL https://aip.scitation.org/doi/10.1063/1.438033.

[7] A. Zhao, L. Shi, Y. Tian, L. Zheng, R. Zheng, Theoretical studies for the infrared spectra of Ar–CO2 complex: Fundamental and combination bands, Spectrochim. Acta A 204 (2018) 308–316, http://dx.doi.org/10.1016/j.saa.2018.06.064, URL https://www.sciencedirect.com/science/article/pii/S1386142518306048.

[8] P.E. Martin, E.F. Barker, The infrared absorption spectrum of carbon dioxide, Phys. Rev. 41 (3) (1932) 291–303, http://dx.doi.org/10.1103/PhysRev.41.291, URL https://link.aps.org/doi/10.1103/PhysRev.41.291.

[9] A. Adel, D.M. Dennison, The infrared spectrum of carbon dioxide. Part I, Phys. Rev. 43 (9) (1933) 716–723, http://dx.doi.org/10.1103/PhysRev.43.716, URL https://link.aps.org/doi/10.1103/PhysRev.43.716.

[10] A. Adel, D.M. Dennison, The infrared spectrum of carbon dioxide. Part II, Phys. Rev. 44 (2) (1933) 99–104, http://dx.doi.org/10.1103/PhysRev.44.99, URL https://link.aps.org/doi/10.1103/PhysRev.44.99.

[11] A. Chedin, The carbon dioxide molecule, J. Mol. Spectrosc. 76 (1–3) (1979) 430–491, http://dx.doi.org/10.1016/0022-2852(79)90236-4, URL http://linkinghub.elsevier.com/retrieve/pii/0022285279902364.

[12] Y.I. Baranov, A.A. Vigasin, Collision-induced absorption by CO2 in the region of ν1, 2ν2, J. Mol. Spectrosc. 193 (2) (1999) 319–325, http://dx.doi.org/10.1006/jmsp.1998.7743, URL http://linkinghub.elsevier.com/retrieve/pii/S0022285298977438.

[13] A.A. Vigasin, Y.I. Baranov, G.V. Chlenova, Temperature variations of the interaction induced absorption of CO2 in the ν1, 2ν2 region: FTIR measurements and dimer contribution, J. Mol. Spectrosc. 213 (1) (2002) 51–56, http://dx.doi.org/10.1006/jmsp.2002.8529, URL http://linkinghub.elsevier.com/retrieve/pii/S0022285202985292.

[14] W.D. Allen, Y. Yamaguchi, A.G. Császár, D.A. Clabo Jr., R.B. Remington, H.F. Schaefer III, A systematic study of molecular vibrational anharmonicity and vibration-rotation interaction by self-consistent-field higher-derivative methods. Linear polyatomic molecules, Chem. Phys. 145 (3) (1990) 427–466, http://dx.doi.org/10.1016/0301-0104(90)87051-C, URL http://linkinghub.elsevier.com/retrieve/pii/030101049087051C.

[15] P.E. Maslen, D. Jayatilaka, S.M. Colwell, R.D. Amos, N.C. Handy, Higher analytic derivatives. II. The fourth derivative of self-consistent-field energy, J. Chem. Phys. 95 (10) (1991) 7409–7417, http://dx.doi.org/10.1063/1.461367, https://doi.org/10.1063/1.461367.

[16] J.M.L. Martin, P.R. Taylor, T.J. Lee, Accurate ab initio quartic force fields for the N2O and CO2 molecules, Chem. Phys. Lett. 205 (6) (1993) 535–542, http://dx.doi.org/10.1016/0009-2614(93)80009-E, URL http://linkinghub.elsevier.com/retrieve/pii/000926149380009E.

[17] H.P. Martins Filho, Molecular orbital anharmonic estimates for the infrared spectrum of CO2, Spectrochim. Acta A 58 (12) (2002) 2621–2632, http://dx.doi.org/10.1016/S1386-1425(02)00006-9, URL http://linkinghub.elsevier.com/retrieve/pii/S1386142502000069.

[18] G. Czakó, T. Furtenbacher, A.G. Császár, V. Szalay, Variational vibrational calculations using high-order anharmonic force fields, Mol. Phys. 102 (23–24) (2004) 2411–2423, http://dx.doi.org/10.1080/0026897042000274991, https://doi.org/10.1080/0026897042000274991.

[19] V. Rodriguez-Garcia, S. Hirata, K. Yagi, K. Hirao, T. Taketsugu, I. Schweigert, M. Tasumi, Fermi Resonance in CO2: a combined electronic coupled-cluster and vibrational configuration-interaction prediction, J. Chem. Phys. 126 (12) (2007) 124303, http://dx.doi.org/10.1063/1.2710256, URL http://eutils.ncbi.nlm.nih.gov/entrez/eutils/elink.fcgi?dbfrom=pubmed&id=17411119&retmode=ref&cmd=prlinks.

[20] S. Maystrovsky, M. Keçeli, O. Sode, Understanding the anharmonic vibrational structure of the carbon dioxide dimer, J. Chem. Phys. 150 (14) (2019) 144302, http://dx.doi.org/10.1063/1.5089460, https://doi.org/10.1063/1.5089460.

[21] B.P. Stoicheff, High Resolution raman spectroscopy of gases: XI. Spectra of CS2 and CO2, Can. J. Phys. 36 (2) (1958) 218–230, http://dx.doi.org/10.1139/p58-026, http://dx.doi.org/10.1139/p58-026.

[22] G. Amat, M. Pimbert, On Fermi resonance in carbon dioxide, J. Mol. Spectrosc. 16 (2) (1965) 278–290, http://dx.doi.org/10.1016/0022-2852(65)90123-2, URL http://linkinghub.elsevier.com/retrieve/pii/0022285265901232.

[23] M.H. Andrade e Silva, G. Amat, Influence of Fermi resonance on the rotational constants of linear triatomic molecules, J. Mol. Spectrosc. 29 (1–3) (1969) 384–401, http://dx.doi.org/10.1016/0022-2852(69)90115-5, URL http://linkinghub.elsevier.com/retrieve/pii/0022285269901155.

[24] H.E. Howard-Lock, B.P. Stoicheff, Raman intensity measurements of the Fermi diad ν_1, $2\nu_2$ in 12CO2 and 13CO2, J. Mol. Spectrosc. 37 (2) (1971) 321–326, http://dx.doi.org/10.1016/0022-2852(71)90302-X, URL http://linkinghub.elsevier.com/retrieve/pii/002228527190302X.

[25] J.F. Bertrán, Study of the Fermi doublet ν_1 — $2\nu_2$ in the Raman spectra of CO2 in different phases, Spectrochim. Acta A 39 (2) (1983) 119–121, http://dx.doi.org/10.1016/0584-8539(83)80066-X, URL http://linkinghub.elsevier.com/retrieve/pii/058485398380066X.

[26] S. Montero, Raman intensities of Fermi diads. I. Overtones in resonance with nondegenerate fundamentals, J. Chem. Phys. 79 (9) (1983) 4091–4100, http://dx.doi.org/10.1063/1.446357.

[27] S.W. Sharpe, R. Sheeks, C. Wittig, R.A. Beaudet, Infrared absorption spectroscopy of CO2-Ar complexes, Chem. Phys. Lett. 151 (3) (1988) 267–272, http://dx.doi.org/10.1016/0009-2614(88)85287-4, URL http://sciencedirect.com/science/article/abs/pii/0009261488852874.

[28] S.W. Sharpe, D. Reifschneider, C. Wittig, R.A. Beaudet, Infrared absorption spectroscopy of the CO2–Ar complex in the 2376 cm−1 combination band region: The intermolecular bend, J. Chem. Phys. 94 (1) (1991) 233–238, http://dx.doi.org/10.1063/1.460380, https://doi.org/10.1063/1.460380.

[29] G.T. Fraser, A.S. Pine, R.D. Suenram, Optothermal-infrared and pulsed-nozzle Fourier-transform microwave spectroscopy of rare gas–CO2 complexes, J. Chem. Phys. 88 (10) (1998) 6157, http://dx.doi.org/10.1063/1.454454, URL https://aip.scitation.org/doi/10.1063/1.454454.

[30] M.W. Severson, Quantum Monte Carlo simulations of Arn–CO2 clusters, J. Chem. Phys. 109 (4) (1998) 1343, http://dx.doi.org/10.1063/1.476686, URL https://aip.scitation.org/doi/abs/10.1063/1.476686.

[31] Y. Ozaki, K. Horiai, T. Konno, H. Uehara, Infrared absorption spectroscopy of Ar–12C18O2: change in the intramolecular potential upon complex formation, Chem. Phys. Lett. 335 (3) (2001) 188–194, http://dx.doi.org/10.1016/S0009-2614(01)00052-5, URL https://www.sciencedirect.com/science/article/pii/S0009261401000525.

[32] Y. Cui, H. Ran, D. Xie, A new potential energy surface and predicted infrared spectra of the Ar–CO2 van der Waals complex, J. Chem. Phys. 130 (22) (2009) 224311, http://dx.doi.org/10.1063/1.3152990, URL https://aip.scitation.org/doi/abs/10.1063/1.3152990.

[33] J.-H. Jung, H. Sun, Vibrational structure and predissociation of Ar-CO2 by CO2 symmetric stretching mode coupled with Ar motion, Bull. Korean Chem. Soc. 23 (2) (2002) 245–252, http://dx.doi.org/10.1137/S0895479898334605, URL http://koreascience.or.kr/article/JAKO200202727392228.page.

[34] T.A. Gartner, A.J. Barclay, A.R.W. McKellar, N. Moazzen-Ahmadi, Symmetry breaking of the bending mode of CO2 in the presence of Ar, Phys. Chem. Chem. Phys. 22 (37) (2020) 21488–21493, http://dx.doi.org/10.1039/D0CP02674C, URL https://pubs.rsc.org/en/content/articlehtml/2020/cp/d0cp02674c.

[35] O. Sode, J.N. Cherry, Development of a flexible-monomer two-body carbon dioxide potential and its application to clusters up to (CO2)13, J. Comput. Chem. 38 (32) (2017) 2763–2774, http://dx.doi.org/10.1002/jcc.25053, http://doi.wiley.com/10.1002/jcc.25053.

[36] J. Ruiz, K. Misa, A. Seshappan, M. Keçeli, O. Sode, Exploring the anharmonic vibrational structure of carbon dioxide trimers, J. Chem. Phys. 154 (14) (2021) 144302, http://dx.doi.org/10.1063/5.0039793, URL https://aip.scitation.org/doi/abs/10.1063/5.0039793.

[37] O. Christiansen, Vibrational structure theory: new vibrational wave function methods for calculation of anharmonic vibrational energies and vibrational contributions to molecular properties, Phys. Chem. Chem. Phys. 9 (23) (2007) 2942–2953, http://dx.doi.org/10.1039/B618764A, URL https://pubs.rsc.org/en/content/articlelanding/2007/CP/B618764A#!divAbstract.

[38] H.J. Werner, P.J. Knowles, G. Knizia, F.R. Manby, M. Schütz, P. Celani, W. Györffy, D. Kats, T. Korona, R. Lindh, A. Mitrushenkov, G. Rauhut, K.R. Shamasundar, T.B. Adler, R.D. Amos, A. Bernhardsson, A. Berning, D.L. Cooper, M.J.O. Deegan, A.J. Dobbyn, F. Eckert, E. Goll, C. Hampel, A. Hesselmann, G. Hetzer, T. Hrenar, G. Jansen, C. Köppl, Y. Liu, A.W. Lloyd, R.A. Mata, A.J. May, S.J. McNicholas, W. Meyer, M.E. Mura, A. Nicklass, D.P. O'Neill, P. Palmieri, D. Peng, K. Pflüger, R. Pitzer, M. Reiher, T. Shiozaki, H. Stoll, A.J. Stone, R. Tarroni, T. Thorsteinsson, M. Wang, MOLPRO, version 2015.1, a package of ab initio programs, 2015.

[39] A.N. Tikhonov, A. Goncharsky, A.G. Yagola, Numerical Methods for the Solution of Ill-Posed Problems, Springer, Netherlands, 1995, URL https://books.google.com/books/about/Numerical_Methods_for_the_Solution_of_Il.html?id=FakIswEACAAJ.

[40] D. Strobusch, C. Scheurer, Hierarchical expansion of the kinetic energy operator in curvilinear coordinates for the vibrational self-consistent field method, J. Chem. Phys. 135 (12) (2011) 124102, http://dx.doi.org/10.1063/1.3637629, URL http://aip.scitation.org/doi/10.1063/1.3637629.

[41] D. Strobusch, C. Scheurer, The hierarchical expansion of the kinetic energy operator in curvilinear coordinates extended to the vibrational configuration interaction method, J. Chem. Phys. 135 (14) (2011) 144101, http://dx.doi.org/10.1063/1.3646514, URL http://aip.scitation.org/doi/10.1063/1.3646514.

[42] J.M. Bowman, Self-consistent field energies and wavefunctions for coupled oscillators, J. Chem. Phys. 68 (2) (1978) 608–610, http://dx.doi.org/10.1063/1.435782, URL http://scitation.aip.org/content/aip/journal/jcp/68/2/10.1063/1.435782.

[43] R.B. Gerber, M.A. Ratner, A semiclassical self-consistent field (SC SCF) approximation for eigenvalues of coupled-vibration systems, Chem. Phys. Lett. 68 (1) (1979) 195–198, http://dx.doi.org/10.1016/0009-2614(79)80099-8, URL http://linkinghub.elsevier.com/retrieve/pii/0009261479800998.

[44] J.M. Bowman, The self-consistent-field approach to polyatomic vibrations, Acc. Chem. Res. 19 (7) (1986) 202–208, http://dx.doi.org/10.1021/ar00127a002, URL http://pubs.acs.org/doi/abs/10.1021/ar00127a002.

[45] M.A. Ratner, R.B. Gerber, Excited vibrational states of polyatomic molecules: the semiclassical self-consistent field approach, J. Phys. Chem. 90 (1) (1986) 20–30, http://dx.doi.org/10.1021/j100273a008, URL http://pubs.acs.org/doi/abs/10.1021/j100273a008.

[46] K.M. Christoffel, J.M. Bowman, Investigations of self-consistent field, scf ci and virtual stateconfiguration interaction vibrational energies for a model three-mode system, Chem. Phys. Lett. 85 (2) (1982) 220–224, http://dx.doi.org/10.1016/0009-2614(82)80335-7, URL http://www.sciencedirect.com/science/article/pii/0009261482803357.

[47] G. Rauhut, Configuration selection as a route towards efficient vibrational configuration interaction calculations, J. Chem. Phys. 127 (18) (2007) 184109, http://dx.doi.org/10.1063/1.2790016, URL http://aip.scitation.org/doi/10.1063/1.2790016.

[48] Y. Scribano, D.M. Benoit, Iterative active-space selection for vibrational configuration interaction calculations using a reduced-coupling VSCF basis, Chem. Phys. Lett. 458 (4–6) (2008) 384–387, http://dx.doi.org/10.1016/j.cplett.2008.05.001, URL http://linkinghub.elsevier.com/retrieve/pii/S0009261408006441.

[49] P.B. Changala, NITROGEN, numerical and iterative techniques for rovibronic energies with general internal coordinates, 2018, URL http://www.colorado.edu/nitrogen.

[50] R.W. Randall, M.A. Walsh, B.J. Howard, Infrared absorption spectroscopy of rare-gas – CO2 clusters produced in supersonic expansions, Faraday Discuss. Chem. Soc. 85 (1988) 13–21, http://dx.doi.org/10.1039/DC9888500013, http://dx.doi.org/10.1039/DC9888500013.